Broadband Sum Frequency Generation Spectroscopy to Study Surface Reaction Kinetics: A Temperature-Programmed Study of CO Oxidation on Pt(111)†

W. G. Roeterdink,‡ J. F. M. Aarts,‡ A. W. Kleyn,‡,§ and M. Bonn*,‡,||

Leiden Institute of Chemistry, Gorleaus Laboratories, Leiden University, P.O. Box 9502, 2300 RA Leiden, The Netherlands, Institute for Plasma Physics Rijnhuizen, P.O. Box 1207, 2430 BE Nieuwegein, The Netherlands, and FOM-Institute for Atomic and Molecular Physics, Kruislaan 407 1098 SJ Amsterdam, The Netherlands

Received: February 20, 2004; In Final Form: April 8, 2004

We demonstrate a novel approach to in-situ monitoring of reaction kinetics on surfaces, using vibrational sum frequency generation (VSFG). In this approach, vibrational spectra of adsorbed molecules are recorded using broadband VSFG as a function of surface temperature. The use of broadband VSFG allows us to obtain spectra of the vibrational resonances over a wide frequency range without tuning the infrared frequency, with good frequency resolution, in small temperature steps. This temperature-programmed vibrational sum frequency generation (TP-VSFG) technique complements conventional temperature-programmed desorption/reaction (TPD/TPR) techniques in that it probes (changes in) the molecules remaining on the surface during the chemical transformation, rather than those ending up in the gas phase. The intensity variations and frequency shifts of the vibrational resonances of surface molecules as chemistry is occurring on the surface contain detailed information on that chemistry. The technique is demonstrated for the benchmark reaction of the catalytic oxidation of carbon monoxide on a Pt(111) surface. Through investigating the temperature-dependent CO stretching vibration, we find that the rate of the oxidation is determined by the oxygen coverage. The activation energy is found to be (0.56 ± 0.05) eV and the preexponential factor is (2.0 ± 0.2) × 10^7 monolayers·s^{-1}, both in excellent agreement with previous measurements.

1. Introduction

The merit of vibrational spectroscopies in the study of surface phenomena is well-established.[1] A number of vibrational techniques provide excellent frequency resolution with submonolayer sensitivity, such as electron energy loss spectroscopy (EELS), reflection absorption infrared spectroscopy (RAIRS), and more recently, infrared−visible vibrational sum frequency generation (VSFG).[2] As the last technique employs short laser pulses (with a duration down to femtoseconds (fs)), it is ideally suited to study the dynamics of surface phenomena, such as inter- and intramolecular energy transfer[3−5] and desorption.[6] One of the advantages of using femtosecond pulses to perform VSFG is that it allows one to sample the surface vibrational spectrum over the bandwidth of the infrared laser pulse (typically 200 cm^{-1}) in a very short time through a multiplexing scheme.[7−9] In this approach complete VSFG spectra can be recorded in a matter of seconds. We make use of that quality here, by continuously monitoring surface vibrational spectra during a temperature ramp.[10] The resulting two-dimensional spectra (vibrational intensity and frequency vs temperature) of this temperature-programmed vibrational sum frequency generation (TP-VSFG) technique contain information on the surface reaction kinetics. This information is clearly complementary to that obtained with conventional temperature-programmed desorption/reaction techniques, as these probe the gas-phase species coming from the surface, whereas TP-VSFG probes what remains on the surface.

We investigate the model system of CO oxidation on the Pt(111) surface, and present a straightforward way of extracting kinetic parameters of a surface reaction from the sum frequency spectra.

Although we present here results under UHV conditions on a single crystal surface, the approach presented in this paper can be extended in a straightforward manner to systems at higher pressures (as has been illustrated previously[11]) and to polycrystalline surfaces,[12] allowing in principle to bridge both the pressure and material gaps. Indeed, VSFG has been successfully applied to investigate the oxidation of CO in a number of studies.[13−16]

The catalytic oxidation of CO on transition metal surfaces has been the focus of many studies (see, e.g., refs 17−20) and forms the basis for the catalytic removal of CO from exhaust gases. Particular attention has been paid to this reaction on the surface of platinum as this is considered to be the benchmark system for the catalytic CO oxidation.[21−25] It is commonly accepted that CO oxidation on the platinum surface occurs through the Langmuir−Hinshelwood mechanism and the activation energy depends on the coverage of both CO and oxygen. The activation energy has been found to be 1.0 eV at low coverage, reduced to 0.5 eV at high coverage.[26] Four oxidation channels (α, β_3, β_2, β_1) have been observed using temperature-programmed desorption (TPD) in combination with time of flight (TOF) mass spectrometry.[27] The α-CO_2 channel (giving rise to the formation of CO_2 at $T = 150$ K in TPD experiments) is correlated with the desorption and dissociation of molecularly chemisorbed oxygen.[23] The β channels correspond to the reactive interaction between adsorbed atomic oxygen and CO admolecules.[24,28] It has been suggested that the β_1 reaction

† Part of the special issue "Gerhard Ertl Festschrift".

* Corresponding author. E-mail: m.bonn@chem.leidenuniv.nl. Fax: 071-5274451.

‡ Leiden University.

§ Institute for Plasma Physics Rijnhuizen.

|| FOM-Institute for Atomic and Molecular Physics.

10.1021/jp049212z CCC: $27.50
Published on Web 05/26/2004

(giving rise to the formation of CO_2 at $T = 330$ K in TPD experiments) proceeds at the perimeters of oxygen islands with mobile adsorbed CO molecules.[24,27,28] More recently, however, Akther et al., have concluded that the oxygen adatoms inside and at the perimeters of the islands are equally reactive to CO so that the β_1 reaction is expected to take place uniformly over the p(2×2)-O islands,[29] which was also suggested by Yoshinobu et al.[30] Kinetic measurements of the CO_2 formation by Xu et al. even suggest a higher reactivity for oxygen atoms inside the island,[31] compared to CO molecules at the perimeter. Using high CO coverage ($\theta_{CO} > 0.25$ monolayer), an additional CO oxidation channel, the β_0 channel at $T = 290$ K, was found by Kostov et al.,[32] suggesting that at these high CO coverages a second CO may be adsorbed per p(2×2)-O unit cell. Electron energy loss spectroscopy (EELS) measurements by Kostov et al.[32] show that at the saturation coverage of oxygen, irrespective of the CO coverage, CO is only adsorbed at the atop sites. Only at temperatures between the β_0 and β_1 (290−330 K) desorption peaks is an electron loss signal observed corresponding to bridged site CO. A possible reaction pathway for the β_1 channel is given in theoretical studies of Glassey et al. and Alavi et al.[33,34] In these studies a p(2×2) overlayer of O atoms is assumed to be adsorbed at the 3-fold hollow sites and the CO molecules are adsorbed at the neighboring atop sites. The CO molecule moves via the bridged site toward the 3-fold hollow site, during which the molecular axis tilts away from the surface normal to approach the OCO angle in CO_2. The reaction barrier, calculated to be 1.3 eV, is determined by the energy required for cleavage of the Pt−O bond.

Scanning tunneling microscopy (STM) confirms the formation of p(2×2) structured islands.[35] The STM measurements showed a lowering of the oxygen atom mobility and a higher degree of ordering of the p(2×2) structure after CO coadsorption. The reaction was monitored while CO was continuously dosed. The surface of the island as a function of time was used to determine the kinetic parameters, resulting among other things in an activation energy of 0.5 eV, in excellent agreement with previous macroscopic measurements,[26] which indicates that the reaction occurs inside the island and not at its perimeters.

We apply the technique of temperature-programmed vibrational sum frequency generation (TP-VSFG) to study CO oxidation on Pt(111). In principle, the resonant VSFG intensity is proportional to the square of the number of surface species, allowing one to directly determine the surface CO coverage. However, for CO on metal surfaces, the situation is more complicated, as the intensity is affected by dipole−dipole coupling, causing deviations from the simple relation. Indeed, Cho et al. have shown that the intensity of the SFG signal and the vibrational frequency scale, to a good approximation, linearly with the coverage for CO on Ru(001),[36] rather than quadratically. An additional complication arises for Pt(111), in that the occupation of bridged sites occurs besides the atop sites, at higher CO coverage. This site dependence will affect the vibrational intensity of the atop site due to intensity transfer between different resonances due to dipole−dipole coupling.[37] These complications can be circumvented by using the vibrational frequency as a probe of surface coverage, rather than integrated intensity. This approach actually makes use of the effect of dipole−dipole coupling, as this causes a marked frequency shift with coverage, which can easily be calibrated.

From our data, we obtain kinetic parameters for the CO_2 channel between 250 and 300 K, $E_a = (0.56 \pm 0.05)$ eV and $A = 2 \times 10^7$ monolayers·s^{-1}, in excellent agreement with previous studies.

2. Experimental Section

The VSFG experiments[38] are performed in an ultrahigh vacuum chamber with a base pressure of 1×10^{-10} mbar. The system is equipped with a mass spectrometer and an electron energy loss spectrometer. Differentially pumped CaF_2 windows serve as entrance and exit ports for the laser radiation. The Platinum crystal is cleaned by sputtering with Ar^+ ions at room temperature, at a current of 3 μA/cm^2, and subsequent annealing to 1200 K. CO is dosed via a leak valve. Thermal desorption spectroscopy is used to calibrate the coverage of the CO molecules. The saturation coverage of CO alone at 273 K is assumed to be 0.5 monolayer.[39] The CO coverage at various exposures is determined from the area under the temperature-programmed desorption (TPD) peak relative to that of the saturation coverage. For the CO oxidation studies, oxygen is first adsorbed to the platinum crystal, followed by the adsorption of CO, both at liquid nitrogen temperatures. The crystal is heated at a constant rate of 0.1 K/s starting at 120 K while SFG spectra averaged over 2 min are accumulated. As the kinetics of the CO oxidation reaction occur over a broad temperature range, it is sufficient to record one spectrum per 12 K temperature increase. If necessary, vibrational spectra can be recorded in a matter of seconds, however.

The laser system used in our experiments is an amplified solid-state Ti:sapphire laser, producing 600 μJ pulses centered around 788 nm (130 fs fwhm, 1 kHz). The major part, 500 μJ, is sent into an optical parametric amplifier (TOPAS), which produces 130 μJ of signal, and an idler, with the signal centered around 1353 nm. After difference mixing of signal and idler in a 2 mm $AgGaS_2$ crystal, 5 μJ at 4785 nm (2090 cm^{-1}) is obtained, with a bandwidth of 200 cm^{-1}. The minor part of the amplifier output is sent into a pulse shaper. The pulse shaper consists of a grating, which angularly disperses the short pulse, and a slit through which only a small part of the spectral bandwidth of the pulse is transmitted to reduce the bandwidth. The resulting upconversion pulse has an energy of 2 μJ of 788 nm with a fwhm of 8 cm^{-1}. A cross-correlation between the infrared and the upconversion pulses typically yields a transient with a width of ~6 ps (fwhm), indicating that the pulse is 3 times transform limited, assuming Gaussian beam profiles. A 20 cm CaF_2 lens is used to focus the upconversion pulse to a fwhm 500 μm focus size, with a spatially Gaussian shaped pulse. The mid-infrared pulse is focused down to a fwhm of 400 μm. The total incident fluence on the crystal never exceeded 2.5 mJ/cm^2, so that heating effects, both single shot and steady state, can be neglected. Variation of the infrared intensity had no effect on the line width of the SFG signal, indicating that saturation effects are negligible.[4] The temporal and spatial overlap on the Pt(111) crystal are found by redirecting both beams into a $LiIO_3$ nonlinear optical crystal outside the vacuum, in which SFG is readily generated. The SFG signal from the CO/Pt(111) system is dispersed by a grating spectrometer and detected with an intensified charge coupled device (CCD) camera.

3. Results

The SFG spectra are accumulated sequentially after dosing various amounts of oxygen and carbon monoxide at 120 K and subsequent heating at a 0.1 K/s rate, as exemplified in Figure 1. The central wavelength of the infrared pulse is tuned to the C−O stretch vibration frequency of CO adsorbed atop Pt atoms, and the SFG intensity therefore reflects the amount of CO molecules adsorbed on these sites.

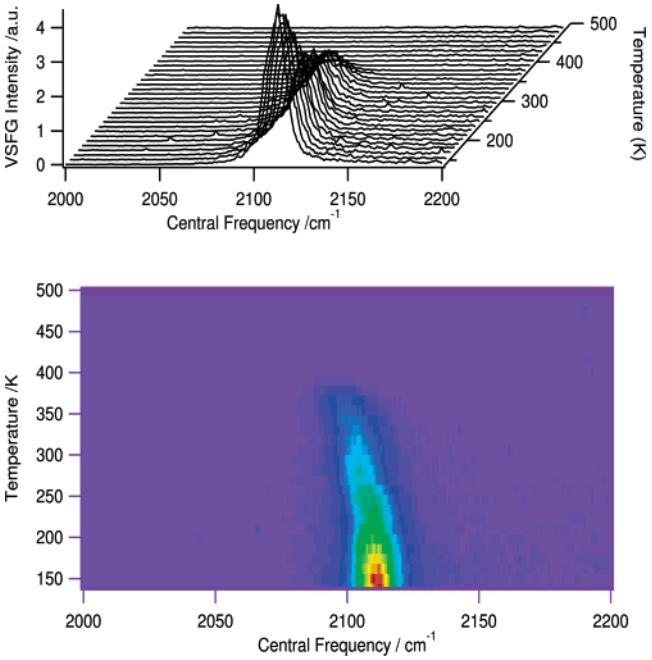

Figure 1. Top panel: sum frequency generation spectra sequentially accumulated after dosing 10 langmuirs of O_2 and 10 langmuirs of CO at 120 K and subsequently heating at a rate of 0.1 K/s. Each SFG spectrum is an average over 120 s. Bottom panel: false color plot of the top figure, with light shades indicating high intensity. This figure clearly shows a frequency shift around 250 K, which can be attributed to CO_2 formation. The frequency shift around 350 K is due to CO desorption.

It is evident from Figure 1 that two effects are observed: a change in SFG intensity and a shift in central frequency. These observations are due to a decrease in CO on the surface, caused by either oxidation and desorption, or a combination of the two. Conventional TPD measurements allow us to distinguish between the two contributions. The TPD results shown in Figure 2 clearly reveal two distinct temperature ranges pertinent to our experiments. Up to 300 K, CO is depleted only through the reaction with coadsorbed oxygen: The CO_2 TPD spectra reveal two reaction channels, the α channel around 150 K (broad, not shown) and a combination of the β_0 and β_1 channels around 280 K. The CO TPD reveals that up to this temperature, desorption of CO does not occur. At 300 K the oxidation reaction is complete—no more CO_2 is formed—and for temperatures exceeding 300 K, desorption of CO occurs. Hence it is clear that the changes in the SFG spectra between 250 and 300 K can be uniquely attributed to the formation of CO_2 and are not related to desorption.

In this article we will focus on the peak in CO_2 production, the β_0/β_1 channels, which we observed around 280 K, shown in Figure 2. A clear shift toward lower temperature is observed with increasing CO coverage, in agreement with TPD measurements by Kostov et al.,[32] who observed the β_1 channel peak at 330 K. Kostov et al. found an extra peak in their TPD spectra at high CO coverage, which was attributed to a new channel, the β_0 channel, at 320 K. Our TPD setup lacks the resolution to see the two channels that are separated by only 10 K. The difference in desorption temperature here and in the previous work of Kostov et al.[32] can be fully accounted for by the different temperature ramps used.

To extract the temperature dependent changes in central frequency and intensity from the data, the SFG spectra are fitted with a sum of a Gaussian line shape for the nonresonant part (labeled *nr*), which is weighted by a phase factor Φ, and a

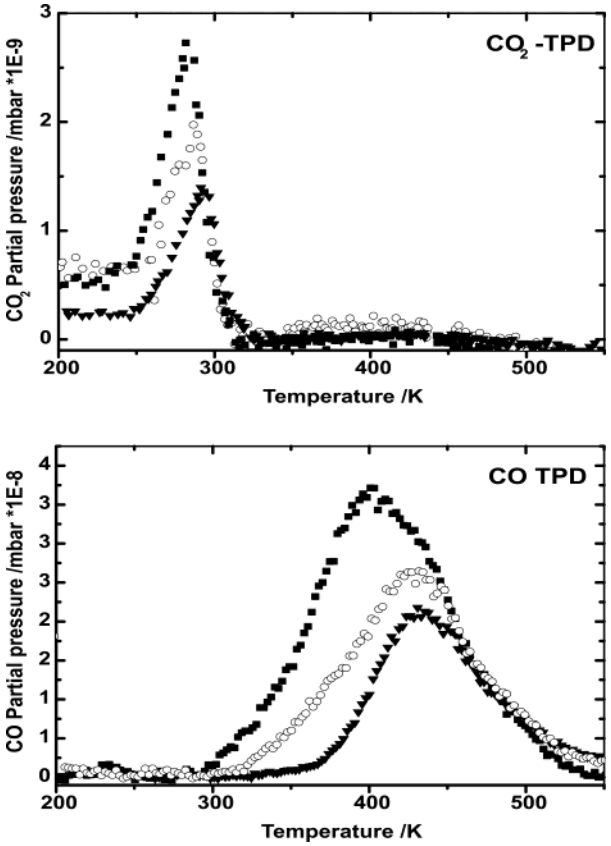

Figure 2. Top panel: thermal desorption spectra (TDS) of the CO_2 production: (■) 10 langmuirs of O_2 + 10 langmuirs of CO; (○) 10 langmuirs of O_2 + 5 langmuirs of CO; (▲) 10 langmuirs of O_2 + 2 langmuirs of CO. Bottom panel: corresponding TDS traces for CO recorded simultaneously with the traces in the upper panel. Note that in the region from 250 to 300 K no CO is desorbing.

Lorentzian line shape for the resonant part (labeled *r*):

$$I_{SFG} \sim |\chi^{(2)}|^2$$

$$\chi^{(2)} = A_{nr}\, e^{-(\omega-\omega_{nr})/Y_{nr}^2} e^{i\Phi} + \frac{A_r}{\omega - \omega_r + i\Gamma_r/2} \qquad (1)$$

$\chi^{(2)}$ is the second-order nonlinear susceptibility, A_{nr} and A_r are the amplitudes of the nonresonant and the resonant signals, respectively, and ω is the frequency of the mid-infrared light. The central frequencies of the Gaussian and Lorentzian contributions are given by ω_{nr} and ω_r, and the widths by Y_{nr} and Γ_r. The central frequency ω_{nr} and the width Y_{nr} of the nonresonant part are determined by the IR pulse characteristics, established independently in a measurement where no CO is present on the crystal. These values are kept fixed while fitting the signals at higher coverage. The phase difference between the resonant and nonresonant contribution, Φ, was chosen to minimize the sum of the errors in the fit for one of the low coverage signals and was kept fixed at this number for all other temperatures.

Figure 3 shows the change in central frequency of the C−O stretch vibration obtained from this fitting procedure, as a function of temperature in the range relevant for the CO oxidation reaction. The observed decrease in central frequency is caused by the decrease in the density of CO molecules as they react with oxygen: the larger average distance between CO molecules, as some are removed to form CO_2, weakens the dipole−dipole interaction between the CO molecules remaining

TABLE 1: Shift in Central Frequency as a Function of Temperature Fitted to a Sigmoidal Boltzmann Function for the Different Oxygen and CO Coverages[a]

O_2 (langmuir)	CO (langmuir)	T_0 (K)	ΔT (K)	ν_i (cm^{-1})	ν_f (cm^{-1})	$\Delta\nu$ (cm^{-1})	$\Delta\theta$(CO) (monolayer)	$\theta(CO)_f$ (monolayer)
10	10	263(1)	13(1)	2103.7(1)	2094.7(2)	9.0	0.16(2)	0.34(3)
10	5	276(1)	9(1)	2100.8(1)	2092.1(2)	8.7	0.15(2)	0.28(3)
10	2	280(1)	10(1)	2096.3(1)	2088.2(2)	8.1	0.13(2)	0.20(2)
7	10	264(7)	12(7)	2101.8(3)	2094.1(7)	7.7	0.12(1)	0.38(3)
7	5	275(1)	9(1)	2100.4(2)	2089.7(3)	8.7	0.15(2)	0.23(2)
5	10	268(4)	18(4)	2101.4(2)	2094.8(4)	6.6	0.08(2)	0.39(3)
5	2	271(1)	8(1)	2095.8(1)	2087.1(2)	6.7	0.08(2)	0.17(2)

[a] The numbers in parentheses give the errors in the last digits. The remaining CO coverage at 330 K, $\theta(CO)_f$, is determined using thermal desorption spectroscopy. One langmuir is defined as 1×10^{-6} mbar·s.

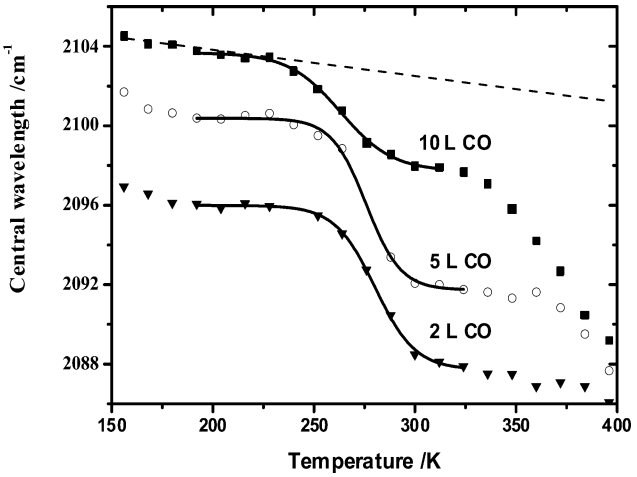

Figure 3. Central frequency as a function of temperature for three different coverages of CO [(top trace, ■) 0.45 monolayer; (middle trace, ○) 0.38 monolayer; (bottom trace, ▲) 0.27 monolayer] all starting with saturation coverage of atomic oxygen (0.25 monolayer). The solid lines represent the fits to the sigmoidal Boltzmann function, eq 3, presented in the text.

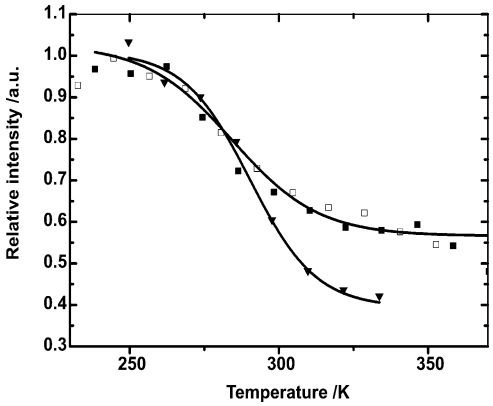

Figure 4. SFG intensity for two different CO coverages as a function of temperature (temperature ramp of 0.1 K/s). CO coverage: (■, □) 0.5 monolayer (10 langmuirs) (illustrating the reproducibility of the approach); (▲) 0.3 monolayer (2 langmuirs). The solid lines represent the fits to the sigmoidal Boltzmann function, eq 3, presented in the text.

on the surface, which is reflected in a frequency shift of the CO stretch vibration.[37] This shift can be calibrated by dosing known amounts of CO at the bare platinum crystal and subsequently determining the central frequency of the SFG signal. This gives a calibration factor of 30 cm^{-1}/monolayer. It was checked that the coverage dependent shift of the vibrational frequency is unaffected by the presence of oxygen. Indeed, varying the amount of oxygen has a very small effect on the CO vibrational frequency, as is evident from the central frequencies of CO for different oxygen coverage as reported in Table 1.

To relate the observed frequency shifts to an absolute change in CO coverage, the shift has to be corrected for the temperature variation during the experiment. It is known from infrared and SFG experiments on CO adsorbed to Pt(111) that there is a small, but nonnegligible, temperature-dependent shift of the vibrational frequency for CO of $\partial\nu/\partial T \approx -0.024$ cm^{-1}/K[3,41,42] due to coupling with the frustrated translation. This temperature shift is assumed to be identical for the CO/O coadsorption system. This is indicated in Figure 3 with a straight, dashed line. In the temperature interval where the oxidation reaction occurs, this trivial temperature-induced shift amounts to 2 cm^{-1}, whereas the shift induced by the oxidation reaction is typically 8 cm^{-1}.

Using the calibrated frequency dependence of the CO coverage, and taking the trivial temperature dependence into account, allows us to determine the amount of CO reacting toward CO_2 as a function of temperature. The change in coverage thus determined is consistent with the amount of CO remaining on the platinum surface following the oxidation reaction, as determined by TPD measurements (i.e., the integrated CO TPD area for $T > 300$ K). The final coverages, i.e., following the oxidation reaction, observed for the different CO dosages are listed in Table 1, in the column $\theta(CO)_f$.

Figure 4 show the integrated SFG intensity as a function of temperature, with a heating rate of 0.1 K/s. The integrated intensity of the resonant part of the SFG signal is roughly linearly dependent on the coverage,[36,43] provided that migration between different sites is negligible. Despite the previously reported linear correlation between SFG intensity and CO coverage, we find that the central frequency is a more reliable and reproducible probe of the coverage than the SFG intensity, as it is insensitive to fluctuations in laser power, and, more importantly, insensitive to migration of CO molecules from atop to bridge sites. This migration process will affect the SFG intensity (as bridge site CO molecules have a vibrational frequency outside our frequency window), but as the dipole−dipole interaction changes only marginally, the vibrational frequency of the atop sites remains largely unaffected. In modeling our data, we will therefore restrict ourselves to the temperature-dependent frequency.

4. Discussion

To derive the reaction parameters, such as the activation energy and the frequency factor, of the catalytic oxidation of CO from our data, the rate equation for the Langmuir−

Hinshelwood mechanism is used:[45]

$$\frac{\partial\theta_{CO}(T)}{\partial T} = -k(T)\theta_{CO}(T)\theta_{O}(T)$$

$$k(T) = A e^{-E_a/kT} \quad (2)$$

in which $\theta_{CO}(T)$ and $\theta_O(T)$ are the CO and O coverages, respectively, at temperature T. The temperature dependence of the reaction rate is assumed to be Arrhenius-like, with A the frequency factor and E_a the activation energy. $\partial\theta_{CO}(T)/\partial T$ and $\theta_{CO}(T)$ can be inferred directly from the CO vibrational frequency as a function of temperature (see Figure 3), as we know the frequency-coverage relation. The frequency shifts ($\Delta\nu$) due to the CO_2 formation are listed in Table 1. The amount of CO oxidized can now be calculated with the help of the change in central frequency $\Delta\nu$ and the calibration factor of 30 cm^{-1}/monolayer; see Table 1. Furthermore, it is evident that the oxygen coverage dependence with temperature $\theta_O(T)$ is identical to the temperature dependence of the CO coverage. This means that in eq 2, all the temperature-dependent variables are determined in the experiment, except for the factor $k(T)$. Using the Arrhenius expression for $k(T)$, this can now be fit to the experimental data, optimizing A and E_a. Taking an average over all the data sets, an activation energy of 0.56 ± 0.05 eV and a preexponential factor of $(2.0 \pm 0.2) \times 10^7$ s^{-1} are derived. These values are in good agreement with previous measurements of Campbell et al.,[26] who used reactive molecular beam-surface scattering, which is a complementary technique (gas-phase) to TP-SFG.

This fitting procedure can be best visualized by considering that an approximate solution to eq 2 is given by the sigmoidal Boltzmann function:

$$\theta_{CO}(T) = \frac{\theta_{CO}(200\text{K}) - \theta_{CO}(330\text{K})}{1 + e^{(T-T_0)/\Delta T}} + \theta_{CO}(330\text{K}) \quad (3)$$

in which $\theta_{CO}(T)$ is the temperature-dependent coverage of CO, T_0 is the temperature at the inflection point, and ΔT is a measure for the rate of the reaction. These coverages are proportional to the SFG frequency, as discussed above. The solid lines in Figure 3 represent the best fits to the data using eq 3. The resulting fit parameters are listed in Table 1. At the highest oxygen dose (10 langmuirs) the temperature at the inflection point T_0 and ΔT are found to be almost independent of the CO coverage, which implies that the oxygen coverage is rate determining. T_0 and ΔT are uniquely related (albeit not analytically) to the two parameters from the Arrhenius expression, A and E_a.

In our analysis, we make use of the fact that the observed CO stretch frequency is dependent on the distance between the CO molecules cubed[37] through dipole−dipole coupling. As this is a very short-ranged interaction, the vibrational frequencies provide a probe of the *very local* environment of the CO molecules: the more CO molecules surrounding one CO, the more blue shifted its vibrational frequency will be. The fact that the frequency of all the CO molecules changes due to CO_2 formation indicates that CO molecules are removed from the surface in a statistical manner. As O islands have been reported on this surface,[35] this means that either the oxidation reaction takes place in the island or, when the reaction occurs at its perimeter, the reacted CO molecules are replaced very quickly by CO molecules from inside the island.

Figure 4 shows the change in SFG intensity as a function of temperature in the temperature range between 250 and 300 K. Following Cho and Harle, one might expect that the SFG intensity scales linearly with CO coverage.[36,43] The curves are fit with a sigmoidal Boltzmann function, for which the fit parameters are listed in Table 2. The initial CO coverage (θ_{CO}(200 K)) is normalized to unity, so that the remaining coverage (θ_{CO}(330 K)) is given as the fraction of the initial coverage. This relative remaining coverage can be directly related to the absolute CO coverage determined from the TPD spectra. The amount of CO converted to CO_2 calculated in that manner is listed in the column $\Delta\theta$(CO) of Table 2. These amounts of reacted CO are higher than those inferred from the SFG frequency shift data. Also the temperatures at the inflection point of the curves do not match with the data inferred from the frequency measurements. These observations illustrate that the integrated intensity is not a good measure of the instantaneous coverage. For CO on Pt(111) this is not very surprising, as changes in the SFG signal around 2100 cm^{-1} in the 250−300 K temperature range are caused not only by CO oxidation but also by migration of molecules from atop sites to bridged sites. This migration has been previously observed in EELS measurements of Kostov et al.[32] As noted above, the central frequency does not suffer from this drawback.

TABLE 2: Parameters Found for the Fit of a Sigmoidal Boltzmann Function (Eq 3) to the SFG Intensity as a Function of Temperature[a]

O_2 (langmuir)	CO (langmuir)	θ_{CO} (220 K)	θ_{CO} (330 K)	T_0 (K)	ΔT (K)	$\Delta\theta$(CO) (monolayer)
10	10	1.00	0.58(5)	277(6)	14(4)	0.25(4)
10	5	1.00	0.46(7)	261(6)	11(2)	0.33(9)
10	2	1.00	0.40(6)	266(4)	18(5)	0.30(8)
7	10	1.00	0.48(2)	286(2)	9(2)	0.41(5)
7	5	1.00	0.28(5)	264(2)	14(2)	0.39(7)
5	10	1.00	0.53(5)	241(5)	5(2)	0.07(1)
5	2	1.00	0.13(5)	268(2)	10(2)	0.54(27)

[a] The numbers in parentheses give the errors in the last digits. One langmuir is defined as 1×10^{-6} mbar·s.

5. Conclusion

We have demonstrated that temperature-programmed vibrational sum frequency generation (TP-SFG) is a useful tool in the in-situ study of reaction kinetics on surfaces. Specifically, for the CO oxidation reaction on the Pt(111) surface, we find that at high coverage of oxygen ($\theta > 0.1$ monolayer) the rate of CO oxidation is independent of the CO coverage, which implies that the Pt−O bond breakage is the rate-determining step. An activation energy of 0.56 ± 0.05 eV and a preexponential factor of $(2.0 \pm 0.2) \times 10^7$ monolayer/s are found, in good agreement with previous studies. The excellent time and frequency resolution of this technique should make it useful to the study of a variety of surface phenomena.

Acknowledgment. We thank Dr. O. Berg for carefully reading the manuscript. This work is part of the research program of the Foundation for Fundamental Research on Matter (FOM), which is financially supported by The Netherlands Organization for Scientific Research (NWO).

References and Notes

(1) Dumas, P.; Weldon, M. K.; Chabal, Y. J.; Williams, G. P. *Surf. Rev. Lett.* **1999**, *6*, 225.

(2) Buck, M.; Himmelhaus, M. J. *Vac. Sci. Technol. A.* **2001**, *19*, 2717.

(3) Beckerle, J. D.; Cavanagh, R. R.; Casassa, M. P.; Heilweil, E. J.; Stephenson, J. C. *J. Chem. Phys.* **1991**, *95*, 5403.

(4) Hess, C.; Wolf, M.; Bonn, M. *Phys. Rev. Lett.* **2000**, *85*, 4341.

(5) Kubota, J.; Yoda, E.; Ishizawa, N.; Wada, A.; Domen, K.; Kano, S. S. *J. Phys. Chem. B* **2003**, *107*, 10329.

(6) Bonn, M.; Hess, C.; Funk, S.; Miners, J. H.; Persson, B. N. J.; Wolf, M.; Ertl, G. *Phys. Rev. Lett.* **2000**, *84*, 4653.
(7) van der Ham, E. W. M.; Vrehen, Q. H. F.; Eliel, E. R. *Surf. Sci*. **1996**, *386*, 96.
(8) Richter, L. J.; Petralli-Mallow, T. P.; Stephenson, J. C. *Opt. Lett.* **1998**, *23*, 1594.
(9) Roke, S.; Kleyn, A. W.; Bonn, M. *Chem. Phys. Lett.* **2003**, *370*, 227.
(10) Denzler, D. N.; Hess, C.; Dudek, R.; Wagner, S.; Frischkorn, C.; Wolf, M.; Ertl, G. *Chem. Phys. Lett.* **2003**, *376*, 618.
(11) Su, X.; Cremer, P. S.; Shen, Y. R.; Somorjai, G. A. *J. Am. Chem. Soc*. **1997**, *119*, 3858.
(12) Kissel-Osterrieder, R.; Behrendt, F.; Warnatz, J.; Metka, U.; Vollp, H.-R.; Wolfrum, J. *Proc. Combust. Inst*. **2000**, *28*, 1341.
(13) Rupprechter, G.; Dellwig, T.; Unterhalt, H.; Freund, H. J. *J. Phys. Chem. B.* **2001**, *105*, 3797.
(14) Chou, K. C.; Markovic, N. M.; Kim, J.; Ross, P. N.; Somorjai, G. A. *J. Phys. Chem. B.* **2003**, *107*, 1840.
(15) Pery, T.; Schweitzer, M. G.; Volpp, H. R.; Wolfrum, J.; Ciossu, L.; Deutschmann, O.; Warnatz, J. *Proc. Combust. Inst.* **2003**, *29*, 973.
(16) Hoffer, S.; Baldelli, S.; Chou, K.; Ross, P.; Somorjai, G. A. *J. Phys. Chem. B.* **2002**, *106*, 6473.
(17) Ertl, G. *Surf. Sci.* **1994**, *299*, 724.
(18) Brown, L. S.; Sibener, S. J. *J. Chem. Phys*. **1989**, *90*, 2807.
(19) Engel, T.; Ertl, G. *J. Chem. Phys.* **1978**, *69*, 1267.
(20) Stampfl, C.; Scheffler, M. *Phys. Rev. Lett.* **1997**, *78*, 1500.
(21) Engel, T.; Ertl, G. *Adv. Catal.* **1979**, *28*, 1.
(22) Eichler, A.; Hafner, J. *Surf. Sci.* **1999**, *433*−*435*, 58.
(23) Matsushima, T. *Surf. Sci.* **1983**, *127*, 403.
(24) Gland, J. L. Kollin, E. B. *Surf. Sci*. **1985**, *151*, 260.
(25) Hendriksen, B. L. M.; Frenken, J. W. M. *Phys. Rev. Lett*. **2002**, *89*, 046101.
(26) Campbell, C. T.; Ertl, G.; Kuipers, H.; Segner, J. *J. Chem. Phys*. **1980**, *73*, 5862.
(27) Allers, K.-H.; Pfnür, H.; Feulner, P.; Menzel, D. *J. Chem. Phys.* **1994**, *100*, 3985.
(28) Gland, J. L.; Kollin, E. B. *J. Chem. Phys*. **1983**, *78*, 963.
(29) Akhter, S.; White, J. M. *Surf. Sci*. **1986**, *171*, 527.
(30) Yoshinobu, J.; Kawai, M. *J. Chem. Phys.* **1995**, *103*, 3220.
(31) Xu, M.; Liu, J.; Zaera, F. *J. Chem. Phys.* **1996**, *104*, 8825.
(32) Kostov, K. L.; Jakob, P.; Menzel, D. *Surf. Sci*. **1997**, *377*, 802.
(33) Glassey, W. V.; Hoffmann, R. *Surf. Sci*. **2001**, *475*, 47.
(34) Alavi, A.; Hu, P.; Deutsch, T.; Silvestrelli, P. L.; Hütter, J. *Phys. Rev. Lett*. **1998**, *80*, 3650.
(35) Wintterlin, J.; Völkening, S.; Janssens, T. V. W.; Zambelli, T.; Ertl, G. *Science* **1997**, *278*, 1931.
(36) Cho, M.; Hess, C.; Bonn, M. *Phys. Rev. B* **2002**, *65*, 205423.
(37) Persson, B. N. J.; Ryberg, R. *Phys. Rev. B* **1981**, *24*, 6954.
(38) Shen, Y. R. *Nature* **1989**, *337*, 519.
(39) Steininger, H.; Lehwald, S.; Ibach, H. *Surf. Sci.* **1982**, *123*, 264.
(40) Schweizer, E.; Persson, B. N. J.; Tüshaus, M.; Hoge, D.; Bradshaw, A. M. *Surf. Sci*. **1989**, *213*, 49.
(41) Roeterdink, W. G.; Berg, O.; Bonn, M. Submitted for publication
(42) Hä, H.; Lehnert, A.; Metka, U.; Volpp, H.-R.; Willms, L.; Wolfrum, J. *Appl. Phys. B* **1999**, *68* (3), 567.
(43) Woodruff, D. P.; Delchar, T. A. *Modern Techniques of Surface Science*; Cambridge Solid State Science Series; Cambridge University Press: Cambridge, UK, 1999.